


Article

Sustained Antibacterial Effect and Wear Behavior of Quaternary Ammonium Contact-Killing Dental Polymers after One-Year of Hydrolytic Degradation

Abdulrahman A. Balhaddad ^{1,2} , Lamia S. Mokeem ¹, Michael D. Weir ^{1,3}, Huakun Xu ^{1,3,*} and Mary Anne S. Melo ^{1,4,*} 

¹ School of Dentistry, University of Maryland, Baltimore, MD 21201, USA; aabalhaddad@umaryland.edu (A.A.B.); lmokeem@umaryland.edu (L.S.M.); MWeir@umaryland.edu (M.D.W.)

² Department of Restorative Dental Sciences, College of Dentistry, Imam Abdulrahman Bin Faisal University, Dammam 34212, Saudi Arabia

³ Biomaterials & Tissue Engineering Division, Department of Advanced Oral Sciences and Therapeutics, University of Maryland School of Dentistry, Baltimore, MD 21201, USA

⁴ Division of Operative Dentistry, Department of General Dentistry, University of Maryland School of Dentistry, Baltimore, MD 21201, USA

* Correspondence: hxu@umaryland.edu (H.X.); mmelo@umaryland.edu (M.A.S.M.)



Citation: Balhaddad, A.A.; Mokeem, L.S.; Weir, M.D.; Xu, H.; Melo, M.A.S. Sustained Antibacterial Effect and Wear Behavior of Quaternary Ammonium Contact-Killing Dental Polymers after One-Year of Hydrolytic Degradation. *Appl. Sci.* **2021**, *11*, 3718. <https://doi.org/10.3390/app11083718>

Academic Editor: Gianrico Spagnuolo

Received: 26 March 2021

Accepted: 14 April 2021

Published: 20 April 2021

Publisher's Note: MDPI stays neutral with regard to jurisdictional claims in published maps and institutional affiliations.



Copyright: © 2021 by the authors. Licensee MDPI, Basel, Switzerland. This article is an open access article distributed under the terms and conditions of the Creative Commons Attribution (CC BY) license (<https://creativecommons.org/licenses/by/4.0/>).

Abstract: This study intended to investigate the long-term antibacterial effect, mechanical performance, and surface topography of new anticaries dental composites. While most artificial aging studies of dental resins lasted for 30–90 days, this study prolonged the water-aging to one year to be more clinically relevant. The base resin was loaded with dimethylaminohexadecyl methacrylate (DMAHDM) at 3 or 5 wt.% and nano-sized amorphous calcium phosphate (NACP) at 20 wt.%. Composites were subjected to one-year water storage and wear. Following water aging, samples were evaluated for flexural strength, elastic modulus, and microbiological assays. Biofilm plate counting method, metabolic assay, colorimetric quantification of lactic acid, and BacLight bacterial viability assay were measured after one year. Topography changes (ΔR_a , ΔR_q , ΔR_v , ΔR_t) were examined after wear and observed by scanning electron microscopy. Biofilm assays and topography changes data were analyzed via one-way ANOVA and Tukey's tests. Mechanical properties and normalized data were verified using a t-test. The flexural strength values for the formulations that contained 5% DMAHDM-20% NACP, 3% DMAHDM, and 5% DMAHDM were reduced significantly ($p < 0.05$) in relation to the baseline but the values were still above the ISO standards. No significant differences were observed between the groups concerning the topography changes, except for the ΔR_t , where there was a significant increase in the 5% DMAHDM-20% NACP group. All the groups demonstrated robust biofilm-inhibition, with slightly reduced antibacterial properties following water aging. The aged samples reduced the total microorganisms, total streptococci, and *mutans streptococci* by 1.5 to 3-log, compared to the experimental control. The new formulations containing DMAHDM and NACP were able to sustain the antibacterial performance after one-year of aging. Mechanical properties and surface topography were slightly affected over time.

Keywords: amorphous calcium phosphate; antibacterial agents; biofilms; dental caries; surface roughness; surface topography

1. Introduction

The most used restorative materials for dental fillings are resin composites. They have excellent aesthetic characteristics, which mimic the natural teeth appearance [1]. Composites require less invasive cavity preparations compared to other restorative materials. However, composites present a reduced lifespan and concerning failure rate in clinical

studies [2–4]. The most common reasons for restorations replacement are secondary caries and restoration fracture [5].

Several investigations have been attempted to defeat this problem by imparting antibacterial additives into composite restorations [6]. However, incorporating antibacterial agents to be released from the materials has shown limited long-term performance. Once the ion release occurs from a booster in the initial weeks to a few months, the amount of discharging decreases over time [7]. The approaches to overcome the limited release and promoted sustained ion release to convey an antibacterial effect are an ongoing investigation area.

Another strategy to convey dental materials with antibacterial properties involves incorporating antibacterial monomers, such as polymerizable quaternary ammonium methacrylates (QAMs), where the antibacterial agent is a component of the polymer matrix, granting the polymer surface with contact-active antibacterial activity [8–10]. Quaternary ammonium methacrylates have been investigated as promising long-lasting antibacterial compounds as they co-polymerize and covalently bond with the other monomers in the composite formulation [8,9].

More recently, dimethylaminohexadecyl methacrylate (DMAHDM) has been synthesized, and its concentration was tuned to induce a high antibacterial effect in preclinical reports [11,12]. The robust antibacterial performance of DMAHDM is attributed to its high surface charge density that can pull toward the negatively charged cell membrane of bacteria. Besides, DMAHDM has a long alkyl-chain that could improve the monomer's penetration capability against the attached microorganisms [11,12].

To complement the antibacterial composites' anticaries strategy, nano-sized amorphous calcium phosphate (NACP) fillers were added to the composite formulations to impart remineralization capabilities [13]. Composites containing NACP fillers release more calcium (Ca) and phosphate (P) ions during the acidic pH challenge [14]. The Ca and P ion release behavior confers buffering capacity and forms a hydroxyapatite layer to remineralize tooth surfaces subjected to demineralization [15–17].

The dual antibacterial and remineralizing formulation with DMAHDM and NACP has been intensively investigated and had demonstrated encouraging immediate anticaries outcomes with no impact on the mechanical or physical properties [15,17]. However, new anticaries composites intended for a clinical application will be subject to aging inside the mouth and exposed to chemical, physical, and mechanical processes [18]. Polymer degradation and aging are among the most intimidating difficulties to the long-term application of new resin-based dental materials [19].

Dental composites are constituted of an organic polymer matrix, usually methacrylate-based monomer and inorganic reinforcing filler particles, commonly glass, quartz, such as alumina, or silica. As the polymer matrix is the resin component of a cured dental resin composite, over time, deterioration is expected with the clinical service [20]. Bonds made between the coupling agent and inorganic filler particles are prone to chemical hydrolysis. This process includes physical reactions such as sorption, dissolution, elution, and physical changes such as softening and swelling [21]. Additionally, the polymer's water sorption and hydrolytic degradation increase material susceptibility to wear during chewing [22]. Previous reports on bioactive composites have focused on short-term effects (up to 180 days) and ion release [23,24].

This study aims to investigate the antibacterial effect, mechanical performance, and surface topography of new anticaries dental composites after one-year water storage and simulated wear. Baseline results were compared to the new results obtained from the long-term evaluation.

2. Materials and Methods

2.1. Experimental Design

Two concentrations of DMAHDM were used (3 and 5 wt.%) in the absence and presence of NACP (20 wt.%) to evaluate their outcomes on the dependent variables. Figure 1 il-

illustrates the design of the study. The designed formulations containing 3 or 5% DMAHDM with and without NACP, the experimental and commercial controls were aged via water-aging for one year or fatigue aging using a chewing simulation machine for 250,000 cycles, equivalent to one year of clinical service under chewing simulation. This experiment was conducted according to a randomized complete block design, with 6 repetitions for each group.

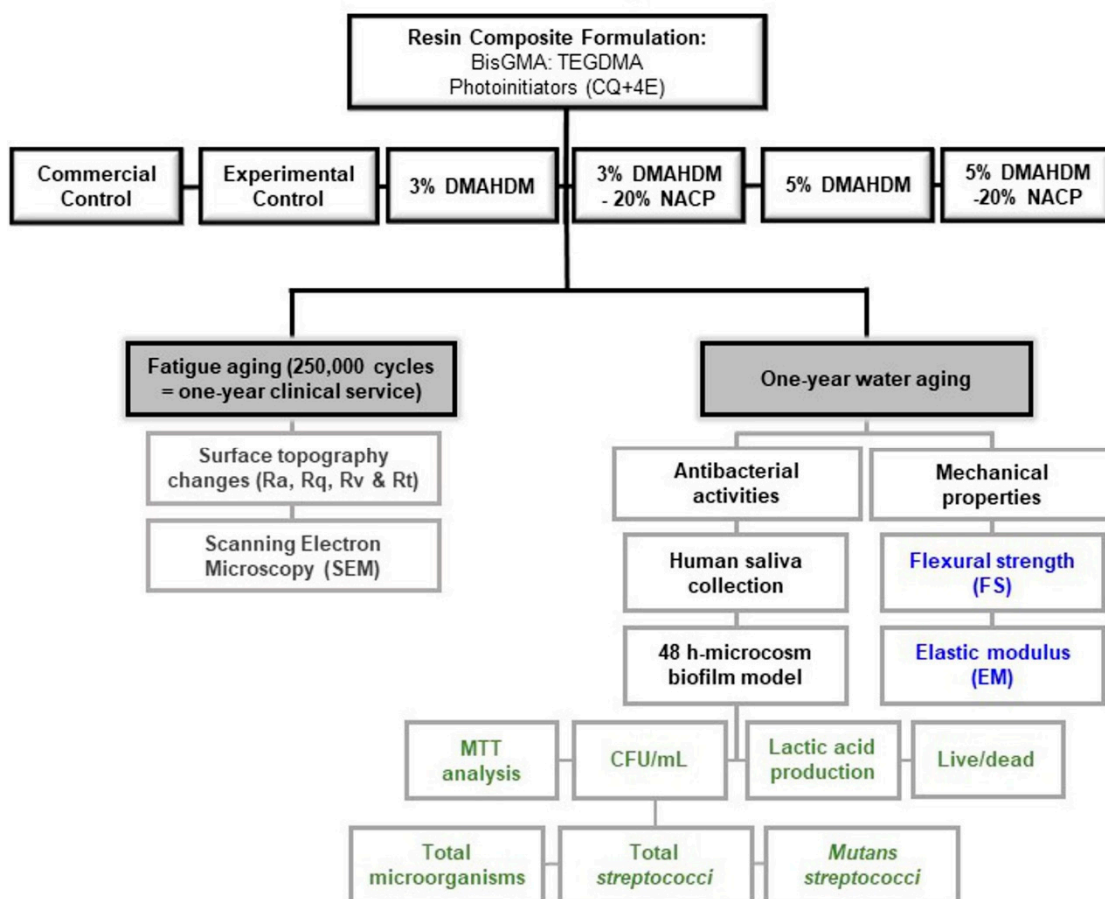


Figure 1. Flowchart of the experimental design proposed in this study. Different antibacterial formulations were designed. Following the aging, the mechanical properties were assessed via flexural strength, elastic modulus, and measurements of the topography changes following simulated wear. The antibacterial activity was analyzed by biofilm plate counting method, metabolic assay, colorimetric quantification of lactic acid, and BacLight[®] bacterial viability assay.

The base resin composed of bisphenol glycidyl dimethacrylate (BisGMA, Esstech, Essington, PA, USA) and triethylene glycol dimethacrylates (TEGDMA, Esstech) at a mass ratio of 1:1. Camphorquinone (0.2 wt.%) and ethyl 4-dimethylaminobenzoate (0.8 wt.%) were used as photoinitiators. Barium boroaluminosilicate glass particles (median size: 1.4 μm ; Dentsply Sirona, Milford, DE, USA) silanized with 4 wt.% 3-methacryloxypropyltrimethoxysilane were incorporated as base fillers.

Then, specimens were divided into the following groups:

1. Commercial control (Heliomolar, Ivoclar Vivadent, Mississauga, ON, Canada): 22% BisGMA and Urethane dimethacrylate resin mix + 77% highly dispersed silicon dioxide, prepolymer, and ytterbium trifluoride as fillers + <1% stabilizers, catalysts, and pigments;
2. Experimental Control: 35% BisGMA-TEGDMA resin mix 1:1 ratio + 65% glass particles;
3. 3% DMAHDM: 32% BisGMA-TEGDMA resin mix 1:1 ratio + 3% DMAHDM + 65% glass particles;

4. 5% DMAHDM: 30% BisGMA-TEGDMA resin mix 1:1 ratio + 5% DMAHDM + 65% glass particles;
5. 3% DMAHDM+20% NACP: 32% BisGMA-TEGDMA resin mix 1:1 ratio + 3% DMAHDM + 20% NACP + 45% glass particles;
6. 5% DMAHDM+20% NACP: 30% BisGMA-TEGDMA resin mix 1:1 ratio + 5% DMAHDM + 20% NACP + 45% glass particles.

2.2. Samples Aging

The samples were immersed in distilled water and stored at 37 °C for one-year of water degrading aging. Following the one-year time, flexural strength and elastic modulus were performed to evaluate the mechanical properties. The antibacterial properties were assessed via biofilm plate counting method, metabolic assay, colorimetric quantification of lactic acid, and BacLight[®] bacterial viability assay. The results were compared to our previous data [15] when the composite samples were tested immediately without aging (referred to as baseline samples).

For the simulated wear, the samples were immersed in artificial chemical saliva prepared according to a previous study [25] and subjected to a chewing simulation machine (Chewing Simulator CS-4, SD Mechatronik GMBH, Feldkirchen-Westerham, Baviera, Germany). The chewing simulation machine is designed to permit appropriate standardization of the number of cycles, speed, load, and frequency against the composite samples. Composite samples were subjected to a load of 49 N, an equivalent of 5 kg, and 250,000 cycles, which is equivalent to almost one year of clinical service [25].

The opposing contact was a steatite tip with 6 mm of diameter (SD Mechatronik, D-83620 Feldkirchen-Westerham, Germany), which was controlled to attain an upward movement of 2 mm, downward movement of 1 mm, horizontal movement of 0.7 mm, speed of upward movement of 40 mm/s, speed of downward movement of 40 mm/s, speed of horizontal movement of 40 mm/s, and frequency of 1 Hz [26]. By the end of the simulated wear, the composite samples' topography changes were investigated via scanning electron microscopy (SEM) and surface roughness instrument.

2.3. Mechanical Properties

2.3.1. Flexural Strength and Elastic Modulus

The samples were prepared using a stainless-steel bar mold ($2 \times 2 \times 25 \text{ mm}^3$). A thin polyester strip was applied on the top of the samples to assure standardization of the surface smoothness [27]. The samples were light-cured (Labolight, DUO, GC, Tokyo, Japan) for 1 min at each side with the radiance emittance of 2330 mW/cm^2 . The samples were kept in water for 15 min before detachment and stored in water for one year. After water aging, the bars were subjected to samples flexural strength and elastic modulus using a three-point flexural test previously described [12].

2.3.2. Surface Roughness and Wear behavior

Composite discs ($\varnothing = 8 \text{ mm}$; 2 mm-thickness) were fabricated using a customized mold and cured (Labolight, DUO, GC, Tokyo, Japan) for 1 min per side to deliver 2330 mW/cm^2 radiant emittance. The surface roughness parameters were noted from the surface exposed to the simulated wear, as described above, using a surface roughness tester (Surftest SJ-310; Mitutoyo America, Aurora, IL, USA). At a sustained speed of 0.5 mm/s, a force of 4 mN, a 0.25-mm cutoff value, and 1.5-mm tracing length, each sample was traversed by the stylus tip ($5 \mu\text{m}$) [28]. An average of five readings from each sample was taken. Then, the following parameters were measured:

- *Average surface roughness (Ra)*: Ra represents the average surface roughness from the roughness profile's mean line.
- *Maximum peak height (Rq)*: denoted as the highest peak produced by the chewing simulation. A high Rq value indicates a high amount of wear.

- *Maximum valley depth (Rv)*: stated as the deepest valley produced by the chewing simulation. A high Rv value indicates a high amount of wear.
- *Maximum high of the profile (Rt)*: Rt estimates the distance between the maximum peak height and the maximum valley depth.

By estimating these roughness parameters before and after the simulated wear, the variation of Ra, Rq, Rv, and Rt for each sample and each group (ΔRa , ΔRq , ΔRv , ΔRt) were calculated. The delta values (Δ) were obtained by subtracting the final values from the initial ones. The results were expressed in μm .

2.3.3. Scanning Electron Microscopy

Following the simulated wear, a representative sample of each group was examined via scanning electron microscopy (SEM). The samples were mounted and gold-sputtered. The composites' surface morphology was then visualized via SEM (Quanta 200, FEI Company, Hillsboro, OR, USA) with 3.5 kV. The representative images were taken at 100, 500, and 1000 \times magnification.

2.4. Microcosm Biofilm Model

Composite discs ($\varnothing = 8$ mm; 0.5 mm-thickness) were fabricated using a customized mold and cured as described above. The discs were stored in water per one day and then stirred for 1 h at 100 rpm using a magnetic bar to release uncured monomers [29]. After one-year of water aging, samples were subjected to a gas diffusion sterilization (ethylene oxide), followed by seven days of de-gassing to guarantee the complete release of entrapped ethylene oxide [30]. The biofilm model used has involved human saliva as inoculum as previously described [15,31–33]. The local Institutional Review Board approved the use of human saliva for in vitro biofilm experiments. The saliva was collected from ten people with healthy oral status. The donors avoided brushing their teeth 24 h and eating or drinking 2 h before saliva collection.

The saliva obtained from each donor was pooled, diluted in sterile glycerol at a 7:3 ratio, and stored at $-80^\circ C$ freezer [15,31–33]. According to the previous report, the saliva-glycerol solution was used as bacterial inoculum mixed with a McBain artificial saliva growth medium at a 1:50 ratio [34]. Next, each composite disc was placed in a 24-well plate well containing the mixed inoculum-growth media and incubated. Growth media was replenished at 8 and 24 after the initial incubation following the protocol described in previous reports [15,31–33]. Biofilm plate counting method, metabolic assay, colorimetric quantification of lactic acid, and BacLight bacterial viability assay were measured in three independent experiments.

2.4.1. Biofilm Plate Counting Method

The biofilm grown over the top of the aged composite discs ($n = 9$) were moved to a vial with 1 mL cysteine peptone water (CPW) for biofilm detachment via sonication and vortex. The biofilm solution was then diluted and plated in one non-selective growth agar (Tryptic soy supplemented with 5% sheep blood) and two selective agar plates (Mitis salivarius agar and Mitis salivarius bacitracin agar) to grow total *streptococci* and *mutans streptococci*, respectively [15,31–33]. After 48 h of incubation, each plate's colony-forming units were counted and expressed as CFU/per disc. The data were then transformed in log 10 for bacterial reduction assessment.

2.4.2. Metabolic Assay

Representative samples of aged composite discs were subjected to a metabolic assay ($n = 9$). This assay is based on metabolically active cells' ability to transform a water-soluble dye[3-(4,5-dimethylthiazol-2-yl) 2,5-diphenyltetrazolium bromide] into an insoluble formazan. The used protocol was described as other else [15].

2.4.3. Colorimetric Quantification of Lactic Acid

The lactic acid produced by the biofilm was quantified via an enzymatic (lactate dehydrogenase) assay. Following the 2-day biofilm formation, representative aged discs ($n = 9$) were submerged into 1.5 mL of buffered peptone water supplemented with 0.2% sucrose. After the 3 h-incubation, the absorbance of the solution in each well was calculated (optical density OD_{340nm}) using the microplate reader. Standard curves were obtained, and results expressed in mmol/L [15,35].

2.4.4. BacLight Bacterial Viability Assay

The viability of the biofilm grown over representative samples of each group was assessed using BacLight kit (Molecular Probes, Eugene, OR, USA). Each sample was stained with a solution of SYTO 9 and propidium iodide (1:1 ratio) for 15 min. Then samples were taken under an inverted epifluorescence microscope (Eclipse TE2000-S, Nikon, Melville, NY, USA). The green fluorescence represents live bacteria's presence, while the red fluorescence indicates the presence of bacteria with defective and compromised bacterial membranes [15,36].

2.5. Statistical Analysis

All experiments were performed with replicates in each of three independent experiments. Normality and equal variance of data were confirmed using the Shapiro-Wilk test. One-way analysis of variance (ANOVA) and Tukey's multiple comparison tests were performed to detect the dependent variables' significant effects on the antibacterial assays and topography changes. Mechanical properties and normalized data of the antibacterial assays before and after aging for each group were compared using the t-test. A p -value < 0.05 was considered statistically significant. All the statistical analyses were performed by Sigma Plot 12.0 (SYSTAT, Chicago, IL, USA).

3. Results

In Figure 2A, the 3% DMAHDM, 5% DMAHDM, and 5% DMAHDM-20% NACP groups had experienced a significant reduction in the flexural strength following the water aging ($p < 0.05$). Although values are acceptable according to ISO 4049 [37]. For the elastic modulus (Figure 2B), experimental control, 3% DMAHDM, 5% DMAHDM, and 3% DMAHDM-20% NACP were increased after aging by around 8% ($p > 0.05$; power of analysis = 100%).

For the biofilm inhibition, the DMAHDM-NACP composites significantly reduced the CFU counts of the total microorganisms' growth in comparison to the control group by 2–3-log ($p > 0.001$; power of analysis = 100%). (Figure 3A). Overall, the log reduction was reduced after aging by around 0.5–1-log using the 5% DMAHDM, 3% DMAHDM-20% NACP, and 5% DMAHDM-20% NACP composites (Figure 3D). For the total *Streptococci*, all the antibacterial formulations resulted in significant inhibition of 1.5–3-log after aging ($p < 0.001$) (Figure 3B). After normalizing the data, the bacterial log reduction demonstrated that the 3% DMAHDM-20% NACP group was the only composite with a significantly reduced antibacterial action by around 1-log (Figure 3E). For *mutans streptococci*, all the formulations significantly ($p < 0.05$) reduced the CFUs after aging ($p < 0.001$). However, (Figure 3F) showed a significant decline of 1–1.5-log of the antibacterial formulations against the *mutans streptococci* CFU.

When analyzing the metabolic activity results, all the antibacterial formulations demonstrated metabolic activity reduction following aging ($p < 0.05$). However, the 5% DMAHDM and 5% DMAHDM-20% NACP groups showed slightly increased activity compared to the baseline samples. When the data were normalized (Figure 4B), the aged samples were found to reduce the metabolic activity by 61–86%, while the baseline samples reduced it by around 68–89%. No significant difference was found between aged and non-aged samples concerning each group after normalizing the data except for the 5% DMAHDM group (Figure 4B).

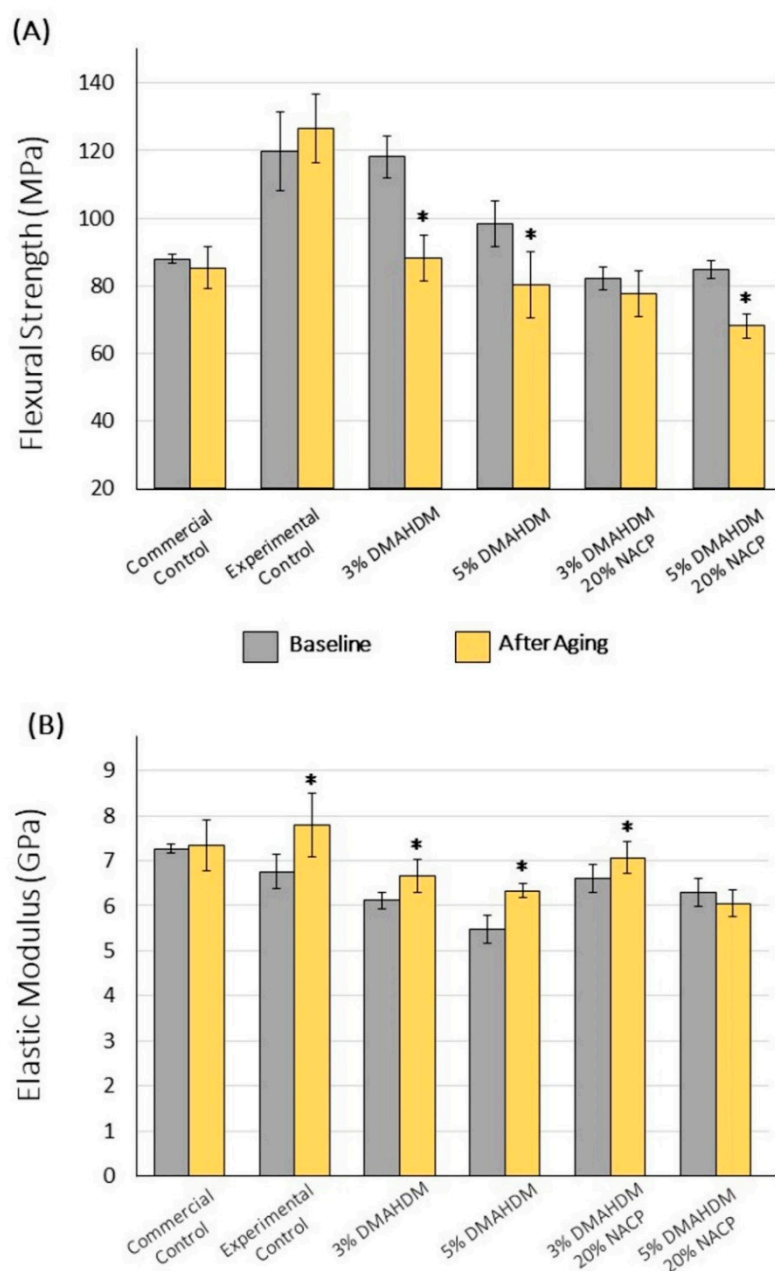


Figure 2. (A) The flexural strength values (mean \pm SD; $n = 6$) of different composite formulations at baseline and after aging. (B) The elastic modulus values (mean \pm SD; $n = 6$) in different composite formulations after aging and at baseline. * Asterisks indicate significant differences compared to baseline values before aging.

For the lactic acid production, the 5% DMAHDM and 5% DMAHDM-20% NACP groups significantly ($p < 0.05$) decreased the lactic acid production after aging compared to the control (Figure 4C). The lactic acid production was slightly increased after aging concerning each antibacterial formulation. The capability of lactic acid inhibition was reduced by around 15–35% (Figure 4D). The 3% DMAHDM is the only group that did not show a reduced inhibition after aging compared to the baseline counterpart ($p > 0.05$).

The live/dead images showed high quantification of viable microorganisms over the experimental control (Figure 5B). The incorporation of 3% and 5% DMAHDM into the composite formulation was associated with a mixture of viable and dead/compromised colonies (Figure 5C,D). Adding 20% of NACP to the DMAHDM was associated with the minor viable microorganisms (Figure 5E,F).

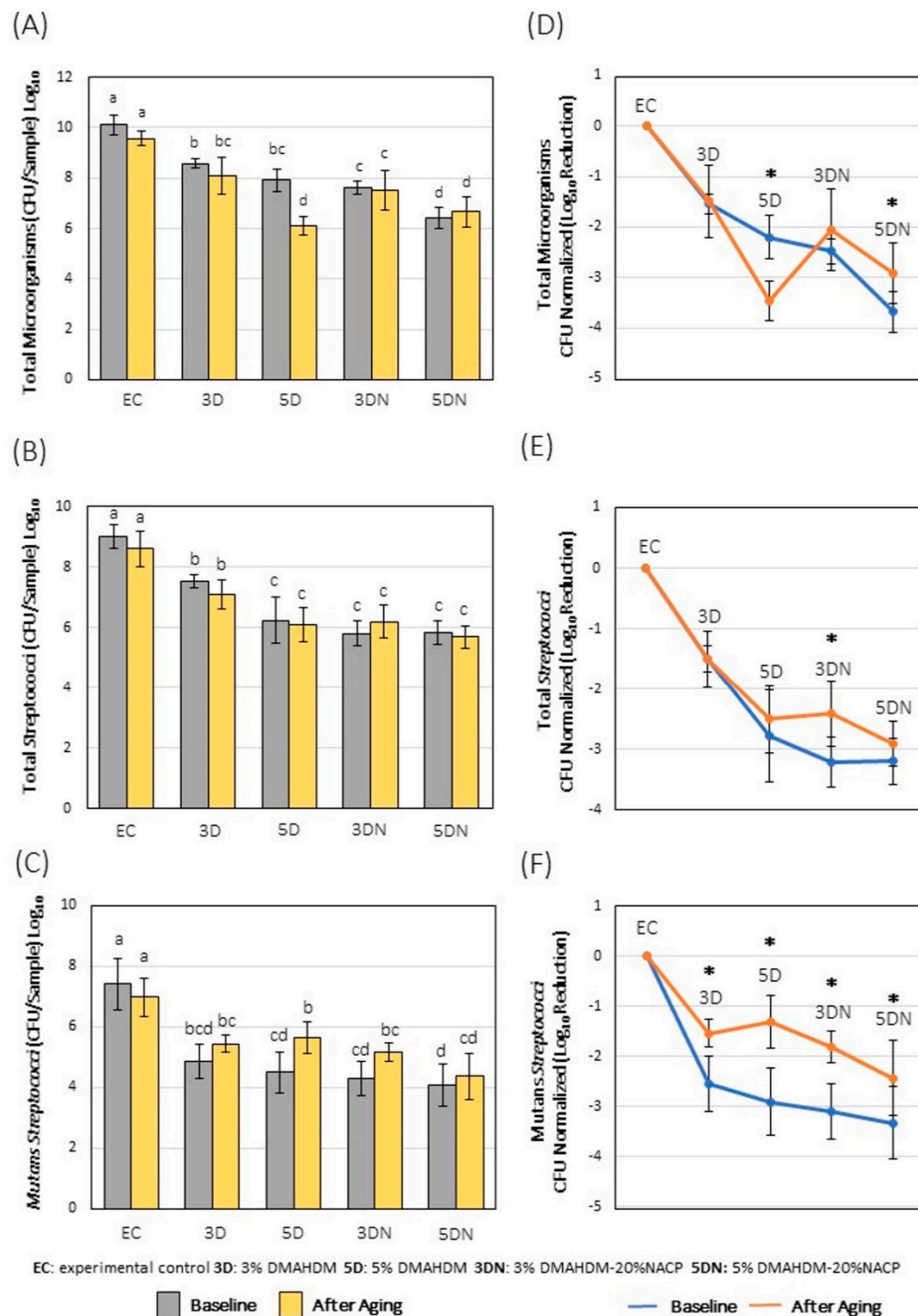


Figure 3. Colony-forming unit (CFU) counts of the (A) total microorganisms, (B) total streptococci, and (C) *mutans streptococci* on the composite surface (mean \pm SD; n = 9). Different letters indicate significant differences between groups ($p < 0.05$). The difference in the log reduction between the baseline and aged samples concerning the (D) total microorganisms, (E) total streptococci, and (F) *mutans streptococci* is illustrated. * Asterisks indicate significant differences compared to baseline values before aging. (EC = experimental control; 3D = 3% DMAHDM; 5D = 5% DMAHDM; 3DN = 3% DMAHDM-20% NACP; 5DN = 5% DMAHDM-20% NACP).

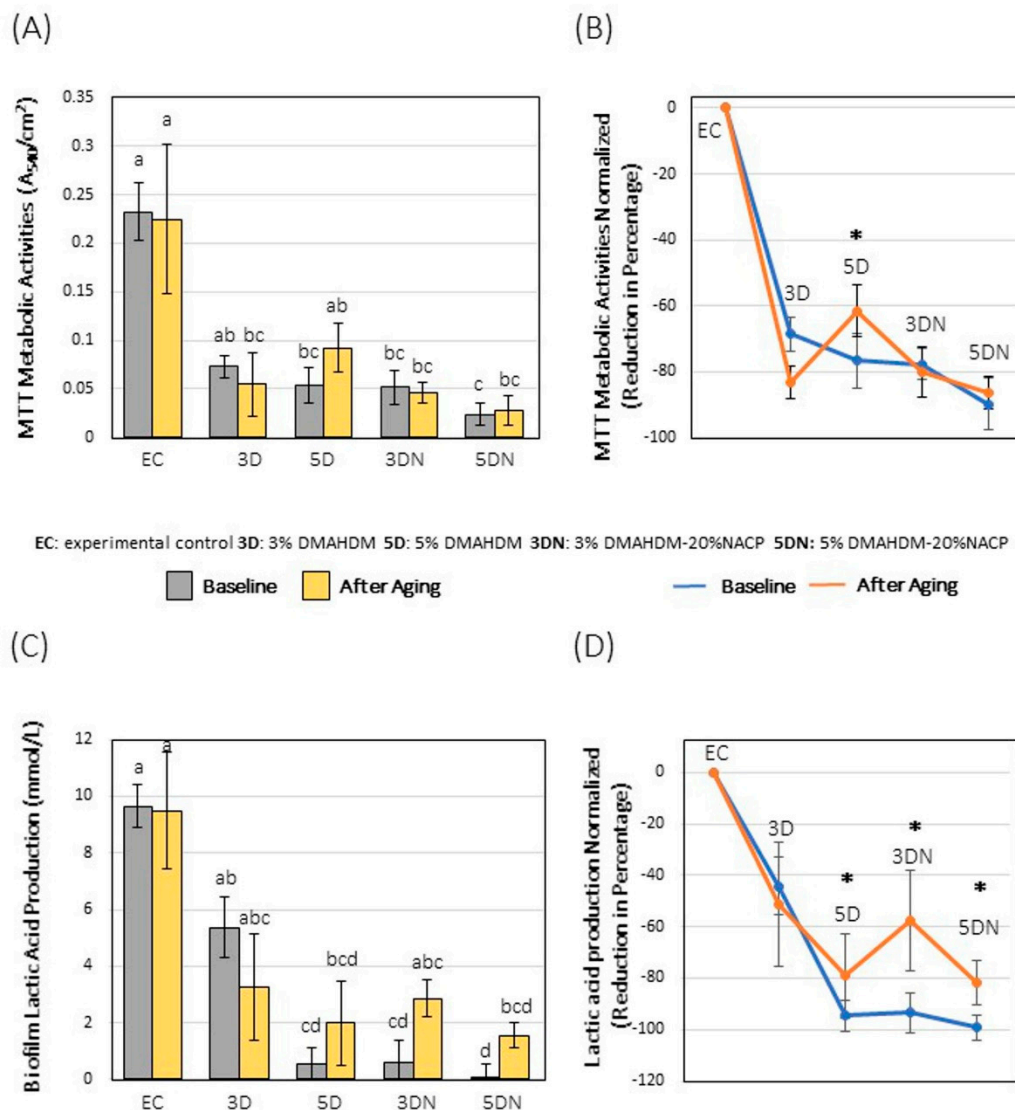


Figure 4. (A) The metabolic activities and (C) lactic acid production of the biofilms grown over the baseline and aged samples (mean \pm SD; $n = 9$). Different letters indicate significant differences between groups ($p < 0.05$). The normalized data of the (B) metabolic activities and (D) lactic acid reduction in percentage. * Asterisks indicate significant differences compared to baseline values before aging. (EC = experimental control; 3D = 3% DMAHDM; 5D = 5% DMAHDM; 3DN = 3% DMAHDM-20% NACP; 5DN = 5% DMAHDM-20% NACP).

Table 1 shows the topography changes following the simulated wear. No significant difference was found between all the groups when the R_a , R_q , and R_v values were observed ($p > 0.05$). However, following the R_t value, the 5% DMAHDM-20% NACP group was significantly associated with more surface discrepancies compared to the experimental control ($p < 0.05$). Figure 6 illustrates the SEM images of the composite samples following the simulated wear. All the investigated groups showed surface topography changes.

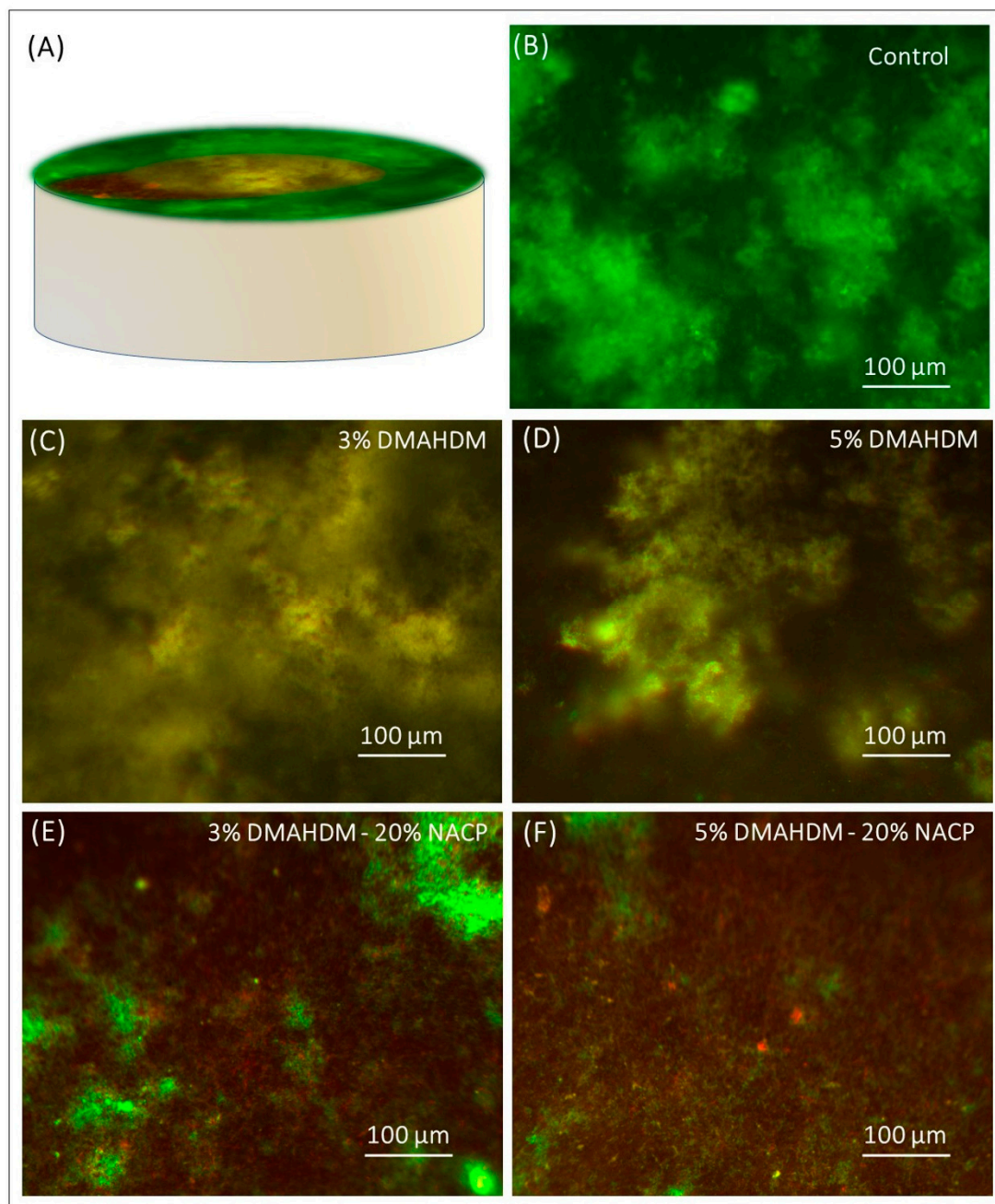


Figure 5. The live/dead images for the biofilms formed over the composites' surface ($n = 3$). (A) A schematic drawing showing the accumulation of the biofilm over the composite surface. Live bacteria were stained green, and compromised bacteria were stained red. The higher amount of viable microorganisms was associated with the experimental control group (B), followed by the 3% and 5% DMAHDM (C,D). The minimum load of viable bacteria was observed over the DMAHDM-NACP groups (E,F).

Table 1. The difference in average surface roughness (ΔRa), maximum peak height (ΔRq), maximum valley depth (ΔRv), and the average distance between the highest peak and lowest valley (ΔRt) of the resin composite formulations subjected to cyclic fatigue (mean \pm SD). Values indicated by different letters are statistically different from each other ($p < 0.05$).

Resin Composite Formulation	Ra (μm)	Rq (μm)	Rv (μm)	Rt (μm)
Commercial Control	0.292 ± 0.098^a	0.189 ± 0.109^a	0.590 ± 0.178^a	1.583 ± 0.429^{ab}
Experimental Control	0.104 ± 0.067^a	0.250 ± 0.107^a	0.221 ± 0.092^a	0.325 ± 0.048^a
3% DMAHDM	0.223 ± 0.145^a	0.307 ± 0.158^a	0.439 ± 0.363^a	1.212 ± 0.627^{ab}
5% DMAHDM	0.310 ± 0.227^a	0.304 ± 0.164^a	0.591 ± 0.549^a	1.674 ± 1.032^{ab}
3% DMAHDM-20% NACP	0.282 ± 0.176^a	0.323 ± 0.180^a	0.604 ± 0.438^a	1.250 ± 1.036^{ab}
5% DMAHDM-20% NACP	0.313 ± 0.166^a	0.388 ± 0.249^a	0.790 ± 0.422^a	2.120 ± 1.537^b

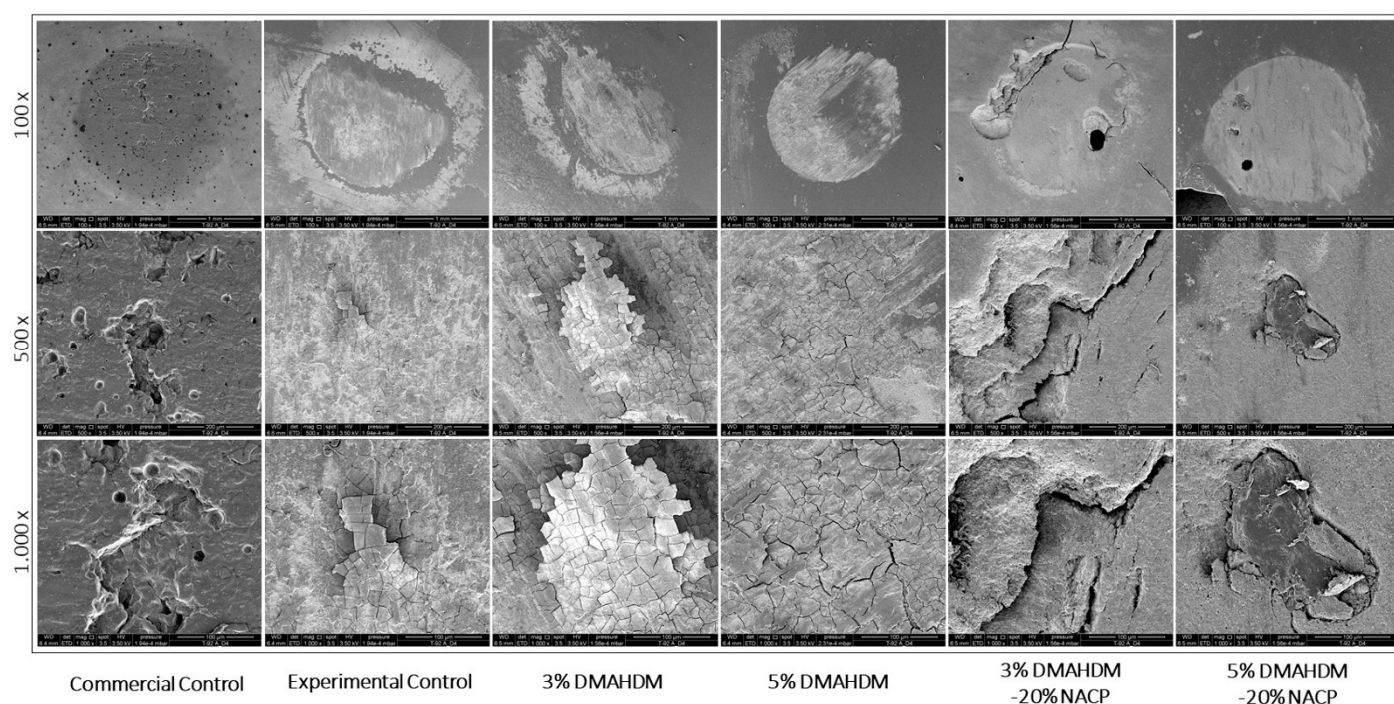


Figure 6. Scanning electron microscopy showing the topography changes on the composites' surfaces following the simulated wear at $\times 100$, $\times 500$, and $\times 1000$ magnification.

4. Discussion

Bioactive composites are constantly being investigated to reduce the risk of treatment failure over time. One drawback of this process is the short-term effect of the materials on bacterial growth [13]. As a result, bioactive dental composites may demonstrate reduced antibacterial properties and weak mechanical performance, threatening their clinical longevity. Early failure of composite restorations may occur due to the breakdown of the resin matrix and its interface with the filler. The hydrolysis of the silane-resin bond could be another mechanism for degradation due to aging [38]. These different degradation patterns may leach the resin matrix and initiate cracks and flaws within the composite's structure, which could deteriorate the restoration's mechanical properties [39].

The degradation and leaching process can chemically and physically change the structure of the composite [18]. Antibacterial formulations with a high rate of degradation and structure changes due to aging are highly expected to lose their bioactivity and strength. As a result, the long-term evaluation of bioactive formulations' antibacterial and mechanical performance is essential before translating them into clinical models.

This study has investigated the impact of water aging on the bioactive composite formulations containing DMAHDM and NACP. Our hypothesis was partially accepted since after one year of water aging; the bioactive formulations demonstrated great antibacterial

action but slightly reduced certain mechanical properties compared to the baseline samples. This present study provides the first outcomes of long-term aging of bioactive composites containing DMAHDM and NACP.

The use of contact-killing monomer in the resin matrix was proposed in 1993 [40]. Since then, several QAMs have been used to impart bioactivity in resin-based materials. DMAHDM, as an antibacterial monomer, has a broad antimicrobial spectrum. Its antibacterial mechanism depends on contact inhibition where the positively charged quaternary amine N^+ sites contact the negatively charged bacterial cell membrane [41]. As a result, the cell membrane will be disrupted, and cytoplasmic leakage will occur [17].

DMAHDM demonstrates more significant biofilm inhibition compared to other QAMs, such as dimethylaminododecyl methacrylate (DMADDM). This might contribute to the long alkyl chain within the DMAHDM structure, which may increase the monomer's contact surface, resulting in more pronounced inhibition. DMAHDM is co-polymerized with the resin matrix via a covalent bond with the polymer network made it immobilized in the composite [42,43]. This characteristic ensures that DMAHDM will constantly attain its antibacterial capability and not collapse over time [40], which was supported by our findings.

Total microorganisms and total streptococci bacterial inhibition showed almost no difference between the baseline and water-aged composite samples. One exception was noticed with the 5% DMAHDM group, where there was about a 2-log difference in reduction on total microorganism in the water-aged samples. On the other hand, *Mutans streptococci* showed less antibacterial effectiveness after aging than the baseline results. *S. mutans* is considered an indicative bacterium related to dental caries due to its capability in acid production, acid tolerance, and the synthesis of intracellular and extracellular polysaccharides [44]. The results suggest that aged samples were less effective against cariogenic bacteria, as the baseline samples were more efficient in killing cariogenic species. This could be attributed to the composite physical changes due to aging, allowing the cariogenic species to adhere more efficiently to the surface than the smooth and non-altered baseline samples. Besides, the resin matrix's leaching may affect the distribution of the DMAHDM over the composite surface, which may compromise the contact killing against the cariogenic species. This explanation could be supported by the fact that DMAHDM has only one methacrylate side [45,46]. As a result, the cross-linking efficiency with other monomers might not be efficient such as dimethacrylate monomers.

There were no significant differences between aged and baseline samples concerning metabolic activities and lactic acid reduction in this study. However, we noticed that the 5% DMAHDM and 5% DMAHDM-20% NACP composites revealed slightly higher metabolic activity after aging. Lactic acid production was also higher in those groups than the 3% DMAHDM-20% NACP compared to baseline samples. This outcome could be correlated to the physiological state of the viable bacterial cells. However, despite the slightly reduced effectiveness, the designed formulations demonstrated potent antibacterial effects following the aging process, indicating these formulations' capabilities to induce repeated antibacterial actions as more biofilm grown over the composite along the time. Although these formulations are promising candidates to prevent secondary caries development, their frequent use may raise questions regarding bacterial resistance. A previous study has addressed this question where the regular exposure to DMAHDM did not induce bacterial resistance against *S. mutans* and other endodontic and periodontal pathogens [47].

It is of utmost importance to evaluate any new product's mechanical properties, predict its performance, and prevent catastrophic failures [48,49]. In dental composites, mechanical properties should be sufficient to function in the oral cavity for an extended period, hopefully encompassing the patient's lifetime [50]. The bioactive composites in this study demonstrated acceptable clinical performance compared to the commercially tested composite before aging.

After one year of aging, the 3% DMAHDM, 5% DMAHDM, and 5% DMAHDM-20% NACP groups showed a significant reduction in flexural strength than their baseline

counterparts. However, the 3% DMAHDM composites showed a higher flexural strength value than the commercial control even after aging. The other groups did not show reduced values than the baseline measurement, but the reduction was not significant. These results may suggest that bioactive composites formulated in this study are mechanically stable. While there is a minor concern related to the 5% DMAHDM-20% NACP group, it might be preferable to limit this group's use in a low-stress area inside the oral cavity, such as cervical and root restorations.

Masticatory load and salivary esterase might affect the surface smoothness of composite restorations inside the oral cavity, which may cause irregularities and physical changes that accelerate the rate of plaque accumulation [51]. Besides, irregularities and physical changes may allow cracks and flaws within the composites, acting as a stress concentration area, facilitating the fracture of such restoration [39]. Hence, it was imperative to evaluate the surface roughness and wear behavior of the bioactive formulations overtime via simulated chewing. In vitro chewing testing provides valuable inputs by simulating clinical settings through masticatory load and artificial saliva [52,53], which assists in the material evaluation.

This study used 250,000 cycles representing one-year clinical service to evaluate our bioactive composites. All the samples reported similar average surface roughness. Particle size, shape, hardness, fillers distribution, properties of the matrix, and the interfacial bonding can influence new formulations' abrasive resistance. Here, the incorporation of the two anticaries agents has not compromised the surface roughness.

No significant differences were also noticed between the R_v and R_q values regarding the wear behavior. Only the R_t parameter, which marks the difference between the maximum peak height and the maximum valley depth, revealed a significant difference between the experimental control and the 5% DMAHDM-20% NACP group, which in line with the finding showing that the 5% DMAHDM-20% NACP group had the lowest flexural strength following aging. This phenomenon could be explained by the resin matrix and its filler interface breakdown due to aging and the degradation that may change the composite's physical structure.

This study is limited to a one-year evaluation for water-based degradation. However, the aging of dental composites inside the mouth is further complex under the influence of saliva, cariogenic biofilms, and patient's diet. In vitro aging models for dental materials evaluate only single factors, missing the complexity of the synergy of factors. The biofilm model used in this study was in static condition with a high concentration of bacterial nutrients, which may allow more biofilm biomass to accumulate over the composites. This static model is different from the dynamic biofilm formation found inside the oral cavity, where saliva's shear force could affect the availability of nutrients [54]. Therefore, complex evaluations are encouraged to obtain clinically relevant information to predict better the performance of new antibacterial and remineralizing dental materials. Besides, future studies may conduct preclinical studies to assess in situ degradation of new anticaries formulations inside the oral cavity. In situ models are highly recommended as a transitional phase to clinical trials. They also extend the knowledge about oral physiological processes, which helps verify the in vitro outcomes [55].

5. Conclusions

Composite materials placed inside the oral cavity are constantly subjected to biofilm formation over their surfaces, contributing to new carious lesions around the restorations. Designing a bioactive antibacterial composite formulation with prolonged antibacterial action and excellent mechanical properties is essential to assure long-term clinical service. Here, we have shown that all the antibacterial formulations substantially reduce biofilm formation even after one year of aging/cycling. Our findings also demonstrated that the antibacterial formulations also maintained acceptable mechanical properties. Overall, this outcome is a step toward designing dental materials that can sustain antibacterial effects over time.

Author Contributions: A.A.B. & L.S.M.: Investigation, Formal analysis, Visualization, Writing—Original Draft. M.D.W.: Investigation, Conceptualization, Writing—Reviewing and Editing. H.X.: Conceptualization, Supervision, Writing—Reviewing and Editing. M.A.S.M.: Conceptualization, Supervision, Writing—Reviewing and Editing. All authors have read and agreed to the published version of the manuscript.

Funding: This work was supported by the University of Maryland School of Dentistry departmental funds (MM, HX).

Institutional Review Board Statement: The study was conducted according to the guidelines of the Declaration of Helsinki, and approved by the Institutional Review Board of University of Maryland Baltimore (HP-00050407, 4 October 2018).

Informed Consent Statement: Informed consent was obtained from all subjects involved in the study.

Data Availability Statement: The data that support the findings of this study are available on request from the corresponding author.

Acknowledgments: The authors are grateful to Esstech (Essington, PA) for kindly donating the BisGMA and TEGDMA monomers. A.A.B. acknowledges the scholarship during his Ph.D. studies from the Imam AbdulRahman bin Faisal University, Dammam, Saudi Arabia, and the Saudi Arabia Cultural Mission.

Conflicts of Interest: The authors (H.X. and M.W.) have patents (US20150299345A1; US8889196B2) to manufacture and use antibacterial monomers and amorphous calcium phosphate nanoparticles used in this study.

References

1. Zhou, X.; Huang, X.; Li, M.; Peng, X.; Wang, S.; Zhou, X.; Cheng, L. Development and status of resin composite as dental restorative materials. *J. Appl. Polym. Sci.* **2019**, *136*, 48180. [\[CrossRef\]](#)
2. Namgung, C.; Rho, Y.J.; Jin, B.H.; Lim, B.S.; Cho, B.-H. A Retrospective Clinical Study of Cervical Restorations: Longevity and Failure-Prognostic Variables. *Oper. Dent.* **2013**, *38*, 376–385. [\[CrossRef\]](#) [\[PubMed\]](#)
3. Kubo, S. Longevity of resin composite restorations. *Jpn. Dent. Sci. Rev.* **2011**, *47*, 43–55. [\[CrossRef\]](#)
4. Van Dijken, J.W.; Pallesen, U. Posterior bulk-filled resin composite restorations: A 5-year randomized controlled clinical study. *J. Dent.* **2016**, *51*, 29–35. [\[CrossRef\]](#) [\[PubMed\]](#)
5. Zhang, N.; Melo, M.A.; Weir, M.D.; Reynolds, M.A.; Bai, Y.; Xu, H.H. Do Dental Resin Composites Accumulate More Oral Biofilms and Plaque than Amalgam and Glass Ionomer Materials? *Materials* **2016**, *9*, 888. [\[CrossRef\]](#)
6. Cocco, A.R.; Rosa, W.L.D.O.D.; da Silva, A.F.; Lund, R.G.; Piva, E. A systematic review about antibacterial monomers used in dental adhesive systems: Current status and further prospects. *Dent. Mater.* **2015**, *31*, 1345–1362. [\[CrossRef\]](#)
7. Pirmoradian, M.; Hooshmand, T. Remineralization and antibacterial capabilities of resin-based dental nanocomposites. In *Applications of Nanocomposite Materials in Dentistry*; Asiri, A.M., Mohammad, A., Eds.; Woodhead Publishing: Cambridge, UK, 2019; pp. 237–269. [\[CrossRef\]](#)
8. Imazato, S. Antibacterial properties of resin composites and dentin bonding systems. *Dent. Mater.* **2003**, *19*, 449–457. [\[CrossRef\]](#)
9. Imazato, S. Bio-active restorative materials with antibacterial effects: New dimension of innovation in restorative dentistry. *Dent. Mater. J.* **2009**, *28*, 11–19. [\[CrossRef\]](#)
10. Antonucci, J.M.; Zeiger, D.N.; Tang, K.; Lin-Gibson, S.; Fowler, B.O.; Lin, N.J. Synthesis and characterization of dimethacrylates containing quaternary ammonium functionalities for dental applications. *Dent. Mater.* **2012**, *28*, 219–228. [\[CrossRef\]](#)
11. Alsahafi, R.; Balhaddad, A.A.; Mitwalli, H.; Ibrahim, M.S.; Melo, M.A.S.; Oates, T.W.; Xu, H.H.; Weir, M.D. Novel Crown Cement Containing Antibacterial Monomer and Calcium Phosphate Nanoparticles. *Nanomaterials* **2020**, *10*, 2001. [\[CrossRef\]](#)
12. Mitwalli, H.; Balhaddad, A.A.; Alsahafi, R.; Oates, T.W.; Melo, M.A.S.; Xu, H.H.K.; Weir, M.D. Novel CaF₂ Nanocomposites with Antibacterial Function and Fluoride and Calcium Ion Release to Inhibit Oral Biofilm and Protect Teeth. *J. Funct. Biomater.* **2020**, *11*, 56. [\[CrossRef\]](#)
13. Balhaddad, A.A.; Kansara, A.A.; Hidan, D.; Weir, M.D.; Xu, H.H.; Melo, M.A.S. Toward dental caries: Exploring nanoparticle-based platforms and calcium phosphate compounds for dental restorative materials. *Bioact. Mater.* **2019**, *4*, 43–55. [\[CrossRef\]](#)
14. Bhadila, G.; Filemban, H.; Wang, X.; Melo, M.A.S.; Arola, D.D.; Tay, F.R.; Oates, T.W.; Weir, M.D.; Sun, J.; Xu, H.H. Bioactive low-shrinkage-stress nanocomposite suppresses *S. mutans* biofilm and preserves tooth dentin hardness. *Acta Biomater.* **2020**, *114*, 146–157. [\[CrossRef\]](#)
15. Balhaddad, A.A.; Ibrahim, M.S.; Weir, M.D.; Xu, H.H.; Melo, M.A.S. Concentration dependence of quaternary ammonium monomer on the design of high-performance bioactive composite for root caries restorations. *Dent. Mater.* **2020**, *36*, e266–e278. [\[CrossRef\]](#)
16. Melo, M.A.; Guedes, S.F.; Xu, H.H.; Rodrigues, L.K. Nanotechnology-based restorative materials for dental caries management. *Trends Biotechnol.* **2013**, *31*, 459–467. [\[CrossRef\]](#) [\[PubMed\]](#)

17. Balhaddad, A.A.; Ibrahim, M.S.; Garcia, I.M.; Collares, F.M.; Weir, M.D.; Xu, H.H.; Melo, M.A.S. Pronounced Effect of Antibacterial Bioactive Dental Composite on Microcosm Biofilms Derived From Patients With Root Carious Lesions. *Front. Mater.* **2020**, *7*. [CrossRef]
18. Szczesio-Wlodarczyk, A.; Sokolowski, J.; Kleczewska, J.; Bociong, K. Ageing of Dental Composites Based on Methacrylate Resins—A Critical Review of the Causes and Method of Assessment. *Polymers* **2020**, *12*, 882. [CrossRef]
19. Krüger, J.; Maletz, R.; Ottl, P.; Warkentin, M. In vitro aging behavior of dental composites considering the influence of filler content, storage media and incubation time. *PLoS ONE* **2018**, *13*, e0195160. [CrossRef] [PubMed]
20. Ferracane, J.L. Resin-based composite performance: Are there some things we can't predict? *Dent. Mater.* **2013**, *29*, 51–58. [CrossRef] [PubMed]
21. Hahnel, S.; Henrich, A.; Bürgers, R.; Handel, G.; Rosentritt, M. Investigation of Mechanical Properties of Modern Dental Composites after Artificial Aging for One Year. *Oper. Dent.* **2010**, *35*, 412–419. [CrossRef] [PubMed]
22. Tsujimoto, A.; Barkmeier, W.W.; Fischer, N.G.; Nojiri, K.; Nagura, Y.; Takamizawa, T.; Latta, M.A.; Miazaki, M. Wear of resin composites: Current insights into underlying mechanisms, evaluation methods and influential factors. *Jpn. Dent. Sci. Rev.* **2018**, *54*, 76–87. [CrossRef]
23. Bhadila, G.; Baras, B.H.; Weir, M.D.; Wang, H.; Melo, M.A.S.; Hack, G.D.; Bai, Y.; Xu, H.H.K. Novel antibacterial calcium phosphate nanocomposite with long-term ion recharge and re-release to inhibit caries. *Dent. Mater. J.* **2020**, *39*, 678–689. [CrossRef]
24. Zhang, N.; Zhang, K.; Melo, M.A.S.; Weir, M.D.; Xu, D.J.; Bai, Y.; Xu, H.H.K. Effects of Long-Term Water-Aging on Novel Anti-Biofilm and Protein-Repellent Dental Composite. *Int. J. Mol. Sci.* **2017**, *18*, 186. [CrossRef] [PubMed]
25. Garcia, I.M.; Balhaddad, A.A.; Aljuboory, N.; Ibrahim, M.S.; Mokeem, L.; Ogubunka, A.; Collares, F.M.; de Melo, M.A.S. Wear Behavior and Surface Quality of Dental Bioactive Ions-Releasing Resins Under Simulated Chewing Conditions. *Front. Oral Health* **2021**, *2*. [CrossRef]
26. Passos, V.F.; Melo, M.A.; Vasconcellos, A.A.; Rodrigues, L.K.A.; Santiago, S.L. Comparison of methods for quantifying dental wear caused by erosion and abrasion. *Microsc. Res. Tech.* **2012**, *76*, 178–183. [CrossRef]
27. ISO E. 4049:2009. *Dentistry-Polymer-Based Restorative Materials*; ISO International Organization for Standardization: Geneva, Switzerland, 2009.
28. Maktabi, H.; Ibrahim, M.; Alkhubaizi, Q.; Weir, M.; Xu, H.; Strassler, H.; Fugolin, A.P.P.; Pfeifer, C.S.; Melo, M.A.S. Underperforming light curing procedures trigger detrimental irradiance-dependent biofilm response on incrementally placed dental composites. *J. Dent.* **2019**, *88*, 103110. [CrossRef] [PubMed]
29. Bhadila, G.; Wang, X.; Zhou, W.; Menon, D.; Melo, M.A.S.; Montaner, S.; Oates, T.W.; Weir, M.D.; Sun, J.; Xu, H.H.K. Novel low-shrinkage-stress nanocomposite with remineralization and antibacterial abilities to protect marginal enamel under biofilm. *J. Dent.* **2020**, *99*, 103406. [CrossRef]
30. Baras, B.H.; Wang, S.; Melo, M.A.S.; Tay, F.; Fouad, A.F.; Arola, D.D.; Weir, M.D.; Xu, H.H. Novel bioactive root canal sealer with antibiofilm and remineralization properties. *J. Dent.* **2019**, *83*, 67–76. [CrossRef]
31. Al-Dulaijan, Y.A.; Cheng, L.; Weir, M.D.; Melo, M.A.S.; Liu, H.; Oates, T.W.; Wang, L.; Xu, H.H. Novel rechargeable calcium phosphate nanocomposite with antibacterial activity to suppress biofilm acids and dental caries. *J. Dent.* **2018**, *72*, 44–52. [CrossRef] [PubMed]
32. Al-Dulaijan, Y.A.; Weir, M.D.; Melo, M.A.S.; Sun, J.; Oates, T.W.; Zhang, K.; Xu, H.H. Protein-repellent nanocomposite with rechargeable calcium and phosphate for long-term ion release. *Dent. Mater.* **2018**, *34*, 1735–1747. [CrossRef]
33. Al-Qarni, F.D.; Tay, F.; Weir, M.D.; Melo, M.A.; Sun, J.; Oates, T.W.; Xie, X.; Xu, H.H. Protein-repelling adhesive resin containing calcium phosphate nanoparticles with repeated ion-recharge and re-releases. *J. Dent.* **2018**, *78*, 91–99. [CrossRef]
34. McBain, A.J. Chapter 4 In Vitro Biofilm Models: An Overview. In *Advances in Applied Microbiology*; Academic Press: Cambridge, MA, USA, 2009; pp. 99–132. [CrossRef]
35. Barker, S. Preparation and colorimetric determination of lactic acid. In *Methods in Enzymology*; Academic Press: Cambridge, MA, USA, 1957; pp. 241–246. [CrossRef]
36. LIVE/DEAD®BacLight™ Bacterial Viability Kit Protocol-US, (n.d.). Available online: <http://www.thermofisher.com/us/en/home/references/protocols/cell-and-tissue-analysis/protocols/live-dead-baclight-bacterial-viability-protocol.html> (accessed on 23 March 2021).
37. ISO 4049:2009-Dentistry-Polymer-Based Restorative Materials, (n.d.). Available online: https://webstore.ansi.org/Standards/ISO/ISO40492009?gclid=EAlaIqobChMI49fVzfQ7wIVGOXIch3o-QogEAAAYASAAEgIIPfD_BwE (accessed on 11 March 2021).
38. Drummond, J.L. Degradation, Fatigue, and Failure of Resin Dental Composite Materials. *J. Dent. Res.* **2008**, *87*, 710–719. [CrossRef] [PubMed]
39. Takeshige, F.; Kawakami, Y.; Hayashi, M.; Ebisu, S. Fatigue behavior of resin composites in aqueous environments. *Dent. Mater.* **2007**, *23*, 893–899. [CrossRef]
40. Mitwalli, H.; Alsahafi, R.; Balhaddad, A.A.; Weir, M.D.; Xu, H.H.K.; Melo, M.A.S. Emerging Contact-Killing Antibacterial Strategies for Developing Anti-Biofilm Dental Polymeric Restorative Materials. *Bioengineering* **2020**, *7*, 83. [CrossRef] [PubMed]
41. Ibrahim, M.S.; Garcia, I.M.; Vila, T.; Balhaddad, A.A.; Collares, F.M.; Weir, M.D.; Xu, H.H.K.; Melo, M.A.S. Multifunctional antibacterial dental sealants suppress biofilms derived from children at high risk of caries. *Biomater. Sci.* **2020**, *8*, 3472–3484. [CrossRef]

42. Makvandi, P.; Jamaledin, R.; Jabbari, M.; Nikfarjam, N.; Borzacchiello, A. Antibacterial quaternary ammonium compounds in dental materials: A systematic review. *Dent. Mater.* **2018**, *34*, 851–867. [\[CrossRef\]](#)
43. Zhang, Y.; Chen, Y.; Hu, Y.; Huang, F.; Xiao, Y. Quaternary ammonium compounds in dental restorative materials. *Dent. Mater. J.* **2018**, *37*, 183–191. [\[CrossRef\]](#)
44. Marsh, P.D. Dental diseases—Are these examples of ecological catastrophes? *Int. J. Dent. Hyg.* **2006**, *4* (Suppl. 1), 3–10, discussion 50–52. [\[CrossRef\]](#)
45. Rego, G.F.; Vidal, M.L.; Viana, G.M.; Cabral, L.M.; Schneider, L.F.J.; Portela, M.B.; Cavalcante, L.M. Antibiofilm properties of model composites containing quaternary ammonium methacrylates after surface texture modification. *Dent. Mater.* **2017**, *33*, 1149–1156. [\[CrossRef\]](#) [\[PubMed\]](#)
46. Vidal, M.L.; Rego, G.F.; Viana, G.M.; Cabral, L.M.; Souza, J.P.B.; Silikas, N.; Schneider, L.F.; Cavalcante, L.M. Physical and chemical properties of model composites containing quaternary ammonium methacrylates. *Dent. Mater.* **2018**, *34*, 143–151. [\[CrossRef\]](#) [\[PubMed\]](#)
47. Wang, S.; Wang, H.; Ren, B.; Li, H.; Weir, M.D.; Zhou, X.; Oates, T.W.; Cheng, L.; Xu, H.H. Do quaternary ammonium monomers induce drug resistance in cariogenic, endodontic and periodontal bacterial species? *Dent. Mater.* **2017**, *33*, 1127–1138. [\[CrossRef\]](#)
48. Sideridou, I.D.; Karabela, M.M.; Vouvoudi, E.C. Physical properties of current dental nanohybrid and nanofill light-cured resin composites. *Dent. Mater.* **2011**, *27*, 598–607. [\[CrossRef\]](#)
49. Rüttermann, S.; Alberts, I.; Raab, W.H.M.; Janda, R.R. Physical properties of self-, dual-, and light-cured direct core materials. *Clin. Oral Investig.* **2010**, *15*, 597–603. [\[CrossRef\]](#)
50. Alzraikat, H.; Burrow, M.F.; Maghaireh, G.A.; Taha, N.A. Nanofilled Resin Composite Properties and Clinical Performance: A Review. *Oper. Dent.* **2018**, *43*, E173–E190. [\[CrossRef\]](#)
51. Fúcio, S.B.; Carvalho, F.G.; Sobrinho, L.C.; Sinhoreti, M.A.; Puppini-Rontani, R.M. The influence of 30-day-old *Streptococcus mutans* biofilm on the surface of esthetic restorative materials—An in vitro study. *J. Dent.* **2008**, *36*, 833–839. [\[CrossRef\]](#) [\[PubMed\]](#)
52. Ionta, F.Q.; Mendonça, F.L.; de Oliveira, G.C.; de Alencar, C.R.B.; Honório, H.M.; Magalhães, A.C.; Rios, D. In vitro assessment of artificial saliva formulations on initial enamel erosion remineralization. *J. Dent.* **2014**, *42*, 175–179. [\[CrossRef\]](#)
53. Sagsoz, O.; Sagsoz, N.P. Chemical degradation of dental CAD/CAM materials. *Bio-Med. Mater. Eng.* **2019**, *30*, 419–426. [\[CrossRef\]](#) [\[PubMed\]](#)
54. Ibrahim, M.S.; Garcia, I.M.; Kensara, A.; Balhaddad, A.A.; Collares, F.M.; Williams, M.A.; Ibrahim, A.S.; Lin, N.J.; Weir, M.D.; Xu, H.H.; et al. How we are assessing the developing antibacterial resin-based dental materials? A scoping review. *J. Dent.* **2020**, *99*, 103369. [\[CrossRef\]](#)
55. Melo, M.A.S.; Weir, M.D.; Passos, V.F.; Rolim, J.P.M.; Lynch, C.D.; Rodrigues, L.K.A.; Xu, H.H.K. Human In Situ Study of the effect of Bis(2-Methacryloyloxyethyl) Dimethylammonium Bromide Immobilized in Dental Composite on Controlling Mature Cariogenic Biofilm. *Int. J. Mol. Sci.* **2018**, *19*, 3443. [\[CrossRef\]](#) [\[PubMed\]](#)